Reaction Cross Sections of U²³³ and U²³⁸ with 18–43-Mev Helium Ions*

J. R. Huizenga, R. Vandenbosch, and H. Warhanek†

Argonne National Laboratory, Argonne, Illinois

(Received August 11, 1961)

The fission cross sections have been measured for U²³³ and U²³⁸ targets bombarded with 18 to 43 Mev helium ions. These targets were chosen because of their large fission cross sections. In addition, the spallation cross sections are known and represent with 43-Mev helium ions only about 4 and 9% of the reaction cross sections of U²³³ and U²³⁸, respectively. The fission fragments were detected with solid-state counters in a small evacuated scattering chamber. The fission fragment counting rates were converted to disintegration rates with previous measurements of the fission fragment angular distributions. The experimental reaction cross sections are in good agreement with reaction cross sections calculated with an optical model in which the complex nuclear potential derived by Igo for alpha-particle elastic scattering is employed. The dependence of the optical model cross sections on the various Woods-Saxon parameters is discussed.

I. INTRODUCTION

IN recent years many experiments[1] have been reported on the elastic scattering of alpha particles from a variety of target nuclei in the energy range up to 50 Mev. These data have been analyzed by several authors, with the objective of determining the strength and spatial extent of the interaction potential between the alpha particle and nucleus. Analyses of the experimental elastic-scattering data in terms of an optical model which expresses the interaction between the alpha particle and nucleus as a complex potential with a diffuse edge have been moderately successful. One of the merits of the optical model is that calculations based on this model also predict total-reaction cross sections.

Total-reaction cross-section measurements for helium-ion projectiles are few in number at this time and those which have been measured are not very accurate. In this paper measurements of total reaction cross sections of U²³³ and U²³⁸ are made to an experimental accuracy of approximately 5%, and these values are compared with optical model cross sections calculated with the complex alpha-particle-nuclear potential determined from analyses of the alpha-particle elastic scattering data. The potential derived by Igo[2] in the energy range up to 50 Mev is given by the expression

$$V+iW=\left\{-1100\exp\left[-\left(\frac{r-1.17A^{\frac{1}{3}}}{0.574}\right)\right]\right.$$

$$\left.-45.7i\exp\left[-\left(\frac{r-1.40A^{\frac{1}{3}}}{0.578}\right)\right]\right\}\text{ Mev.}\quad(1)$$

Since the elastic scattering data defines the complex potential near the nuclear surface (and does not give information on the potential for small values of r), the above expression is valid only for large values of r where the absolute value of the real part of the potential is less than 10 Mev.

The total reaction cross sections reported here were obtained by summing the combined excitation functions of all reaction products. The targets U²³³ and U²³⁸ were chosen because of their large fission cross sections. In addition, the spallation cross sections are known and represent with 43-Mev helium ions only about 4% and 9% of the reaction cross sections of U²³³ and U²³⁸, respectively. The fission cross sections of these targets make up most of the reaction cross sections and are measured with good accuracy by a technique which utilizes solid state counters for detecting the fission fragments. Therefore, the errors associated with usual difficulties encountered in measuring reaction cross sections by summing excitation functions of all possible reaction products, such as missing excitation functions and uncertainties in absolute counting efficiencies of the product nuclei, are minimized in these experiments. Although a transmission method for measuring the total reaction cross section has been applied to proton-induced reactions,[3] no similar measurement has been reported for helium-ion projectiles.

The information on total reaction cross sections with helium-ion projectiles which is obtained by summing excitation function data is discussed by Igo.[2] One of the more accurate measurements of reaction cross sections comes from the excitation functions of bismuth[4,5] where the final products of large yield are alpha-emitting isotopes. The probability for proton emission is small and the total-reaction cross section is fairly well represented by the sum of the Bi²⁰⁹(α,xn) At⁽²¹³⁻ˣ⁾-reaction cross sections. The Bi²⁰⁹(α,n) excitation function is, however, not known.

The first helium-ion-induced fission cross-section measurements obtained with a counter technique were reported by Jungerman.[6] He detected the fission pulses

[1] References to the literature in this field are contained in a review article by R. M. Eisberg and C. E. Porter, Revs. Modern Phys. **33**, 190 (1961).

[2] G. Igo, Phys. Rev. **115**, 1665 (1959).

[3] R. M. Eisberg, *Proceedings of the International Conference on the Nuclear Model, 1959* (The Research Council, Florida State University, Tallahassee, Florida, 1959); G. W. Greenlees and O. N. Jarvis, *Proceedings of the International Conference on Nuclear Structure, Kingston* (University of Toronto Press, Toronto, 1960); N. M. Hintz (private communication).

[4] E. L. Kelly and E. Segrè, Phys. Rev. **75**, 999 (1949).

[5] W. J. Ramler, J. Wing, D. J. Henderson, and J. R. Huizenga, Phys. Rev. **114**, 154 (1959).

[6] J. Jungerman, Phys. Rev. **79**, 632 (1950).

in an ionization chamber in the presence of the ionization produced by the beam itself by use of a cancellation technique. The helium-ion-induced fission cross sections of Jungerman[6] are smaller than our values by a factor of 2, and this discrepancy may be related to unreliable operation of the ionization chamber in the early work of Jungerman as discussed by Steiner and Jungerman.[7] Several measurements of total fission cross sections with helium-ion projectiles have been made by radiochemical techniques.[8-12] This method necessitates the addition of the excitation functions of many final fission products. Among the difficulties inherent in the radiochemical fission cross-section measurements are assumptions about the charge distribution, uncertainties in the estimates of the cross sections for the mass chains which are not experimentally measured, incomplete and erroneous decay scheme data, and the problems associated with absolute beta and gamma counting. The radiochemical fission cross sections are in reasonable agreement with our solid-state counter results, however, the fission cross section measurements[12] for which the greatest amount of attention was paid to factors such as absolute beta and gamma counting give values which are approximately 15% smaller than our values.

II. EXPERIMENTAL PROCEDURE

A. Target Preparation

The U^{238} targets were prepared by volatilization of 50 to 200 μg of heavy element per square centimeter onto 0.0005- to 0.001-in. aluminum backing foils. The area of the uranium deposit was fixed by a collimator of known diameter and the mass of U^{238} was determined by alpha particle counting in conjunction with an alpha pulse height analysis. The U^{238} was highly depleted in U^{235} and U^{234} and had an isotopic content of greater than 99.99%. The U^{238} targets were very uniform in thickness.

The U^{233} targets were prepared by electrodeposition of 75 to 125 μg of heavy element per square centimeter onto 0.001-in. aluminum backing foils. The U^{233} had an isotopic composition of 98.3% U^{233}, 0.13% U^{234}, 0.01% U^{235} and 1.53% U^{238}. The mass of U^{233} was measured by masking the uranium plate with a collimator of known area and counting the alpha particles in a low-geometry counter. Alpha pulse-height analysis indicated that essentially all the alpha activity was due to U^{233}. The deposits were tested for uniformity and found to be uniform to within about 10%.

B. Energy-Degrading System and Scattering Chamber

The energy-degrading system and scattering chamber have been described in a previous publication.[13] The energy of the helium ions emerging from the Argonne constant-frequency cyclotron are degraded to the desired energy by aluminum foils of the proper thickness. The details of the energy-degrading focusing system are described[14] elsewhere. The measured mean ranges of the beam were converted to helium-ion energies with the range-energy relation determined for protons[15] and the assumption that the energy loss of different particles has the same velocity dependence $F(v)$ so that $R = (M/Z^2)F(v)$.

The beam is refocused after passing through the degrading foil and after traversing some distance passes through a 7-ft wall and enters an experimental area in which the 11-in.-diam scattering chamber is located. The beam is controlled in the experimental area with focusing and deflection coils. The collimating system restricts the diameter of the beam at the target to $\frac{1}{8}$ in.

C. Fission Fragment Detectors

The solid-state detectors are similar to those used in the study[13] of the fission fragment angular distributions of heavy elements. The detectors were placed directly back of collimators of known area in order to establish the solid angle. The collimators were located 4 inches from the fissionable target. Collimators of three known diameters which varied in area by approximately a factor of 10 were used to establish the uniformity of response of different areas of the detectors to fission fragments. In most of the experimental runs the collimators of largest size (0.3 cm^2) were used.

D. Electronics

The electronic system used in these experiments is similar to that described[13] previously. The signals from the solid-state detectors were amplified by a factor of 50 with preamplifiers which were attached to the scattering chamber. The outputs from the preamplifiers were relayed to the counting area by cables which are approximately 150 ft long. The pulses were amplified and then fed into single-channel analyzers that were used as integral discriminators. Their discriminator levels were adjusted so as to discriminate against most of the pileup pulses caused by scattered alpha particles. Using the output pulses of the single-channel analyzers as gating pulses it was then possible to prevent the 256-channel analyzer from sorting the low-energy pulses, thus reducing the deadtime of the analyzer. Through use of scalers the single-channel analyzers also

[7] H. M. Steiner and J. A. Jungerman, Phys. Rev. **101**, 807 (1956).

[8] R. A. Glass, R. J. Carr, J. W. Cobble, and G. T. Seaborg, Phys. Rev. **104**, 434 (1956).

[9] R. Vandenbosch, T. D. Thomas, S. E. Vandenbosch, R. A. Glass, and G. T. Seaborg, Phys. Rev. **111**, 1358 (1958).

[10] B. M. Foreman, Jr., W. M. Gibson, R. A. Glass, and G. T. Seaborg, Phys. Rev. **116**, 382 (1959).

[11] R. Gunnink and J. W. Cobble, Phys. Rev. **115**, 1247 (1959).

[12] L. J. Colby, Jr., M. L. Shoaf, and J. W. Cobble, Phys. Rev. **121**, 1415 (1961).

[13] R. Vandenbosch, H. Warhanek, and J. R. Huizenga (to be published).

[14] W. J. Ramler, J. L. Yntema and M. Oselka, Nuclear Instr. and Methods **8**, 217 (1960).

[15] H. Bichsel, Phys. Rev. **112**, 1089 (1958); H. Bichsel, R. F. Mozley, and W. A. Aron, *ibid.* **105**, 1788 (1955).
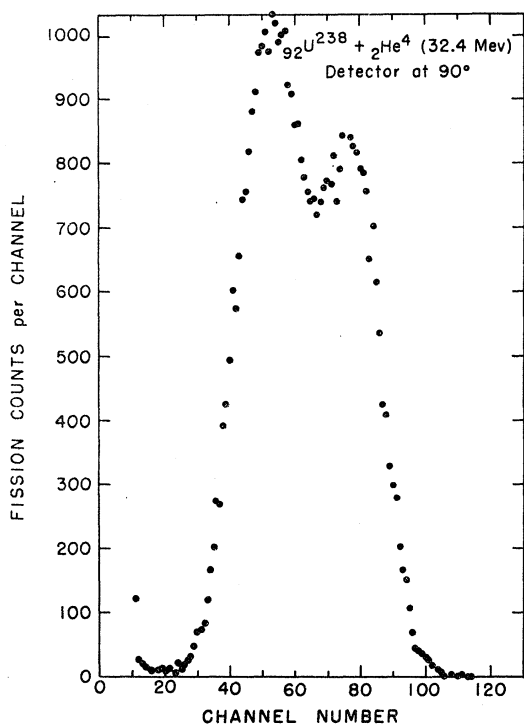
FIG. 1. Energy spectrum of fission fragments obtained with solid-state detectors and recorded in a multichannel analyzer. The low-energy pulses (below channel 10) from noise and scattered alpha particles are eliminated from the multichannel analyzer by a technique described in text.

allowed a quick check on the counting rates of the two detectors. The signals from the two amplifiers were fed into alternate halves of the 256-channel analyzer, utilizing a routing pulse from a discriminator circuit in one of the amplifiers.

The total number of helium ions striking the target was measured with a Faraday cup and a vibrating reed electrometer the output of which was fed to an integrator. The over-all accuracy of the integrated beam current from this system is about 1%.

III. EXPERIMENTAL RESULTS

The fission-fragment counting rates were determined with solid-state detectors at two angles simultaneously, the angles of the detectors usually being 90° and 174° to the beam direction with the fissionable layer of material on the cyclotron side of the backing foil. In most of the experiments the fissionable target was placed at an angle such that the normal to the target bisects the angle between the two detectors. The fissionable targets were thin enough such that self-absorption was completely negligible in our counting arrangement. This fact was established by changing the angle of the target from the above position to positions where the normal to the target was first moved 30° toward one detector and then 30° toward the second detector and observing no differences in the measured ratios of the counting rates for the two detectors.

The length of each experiment was such that the

statistical uncertainty in the number of fission counts collected was less than 1% for helium ions of energies greater than 25 Mev, less than 2% for helium ions of energy between 20 and 25 Mev and of order of 10% for helium ions of energy less than 20 Mev. The range of the emergent helium ions was measured in conjunction with each cross section determination. During some of the low-energy runs, for which the elapsed time was of the order of one hour, the accelerating conditions of the cyclotron shifted sufficiently to change the range of the emergent helium ions by an amount up to 1.0 mg/cm². With an absorber which reduces the energy of the initial beam to 20 Mev the above uncertainty introduces an uncertainty of about $\frac{1}{4}$ Mev in bombarding energy.

The number of fission fragment counts for a fixed helium ion current was determined by integrating the number of pulses in the fission fragment spectrum as observed with a multichannel analyzer. The valley between fission fragment pulses and the much smaller pulses due to scattered alpha particles and noise is illustrated in Fig. 1. By adjusting the discriminator levels in the single-channel analyzers and making use of gating pulses it was possible to eliminate the low-energy pulses from the multichannel analyzer. In the spectrum shown in Fig. 1, for example, the discriminator eliminated pulses with energy such that they would fall in the first 10 channels without the coincidence operation. The helium ion current on the target was adjusted to give a fission counting rate small enough so that the dead time correction of the multichannel analyzer was less than 1%.
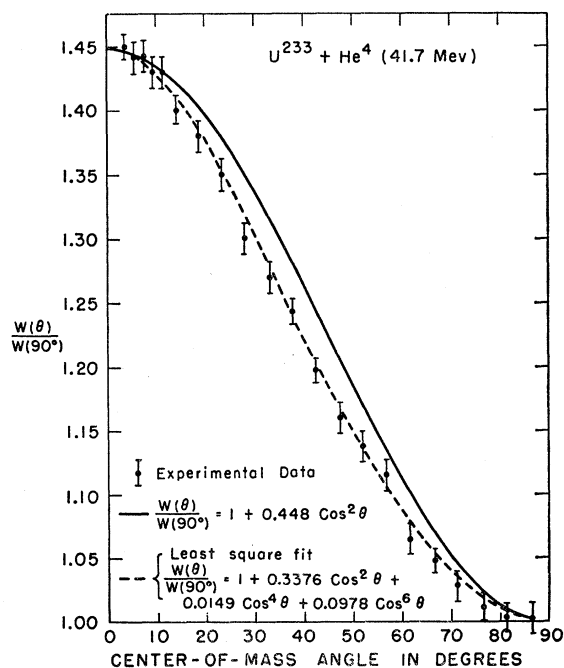

FIG. 2. Angular distribution of fission fragments. The solid-line curve is drawn to give the same $W(6°)/W(90°)$ intensity ratio.

The fission cross sections were calculated by integrating the measured differential fission cross sections over 2π solid angle since two fragments are formed per fission event. The expression which is integrated contains a factor which accounts for the fission fragment anisotropy. The experimental fission fragment angular distributions, where one detector is kept at a fixed angle and the second detector moved to many angles between 90° and 180° (or 0°), have been measured[13] for U²³³ and U²³⁸ at two bombarding energies. A typical distribution is shown in Fig. 2. The experimental data are fitted by a least-squares technique with Legendre polynomials having terms up to $P_6(\cos\theta)$. These angular distributions were used in the fission cross section calculations rather than the simple $a+b\cos^2\theta$ angular distributions. The experimental fission fragment angular distributions resulting from a 41.7-Mev helium-ion bombardment of U²³³ is shown in Fig. 2 along with two theoretical curves which give the same value of the fission fragment intensity ratio at 6° and 90°, i.e., $\omega(6°)/\omega(90°)$. The more simple expression, $\omega(\theta)/\omega(90°)=1+0.448\cos^2\theta$, leads to a fission cross section which is 7% larger than the second expression

$$\omega(\theta)/\omega(90°)=1+0.3376\cos^2\theta+0.0149$$
$$\times\cos^4\theta+0.0978\cos^6\theta,$$

which fits the experimental points at all angles. For a bombarding energy of 32 Mev the distribution given by $a+b\cos^2\theta$, and normalized to the experimental angular distribution at 6° and 90°, gives a fission cross
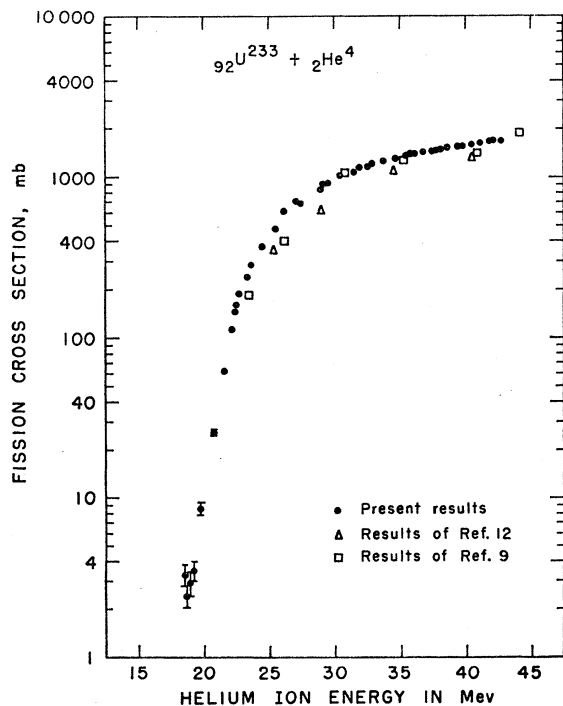

FIG. 3. Experimental fission cross sections of U²³³ as a function of helium-ion energy in the laboratory system. The solid points are the results obtained with solid-state detectors and the triangles and squares are earlier radiochemical measurements.

FIG. 4. Experimental fission cross sections of U²³⁸ as a function of helium-ion energy in the laboratory system. The solid points are the results obtained with solid-state detectors and the triangles and squares are earlier radiochemical measurements.
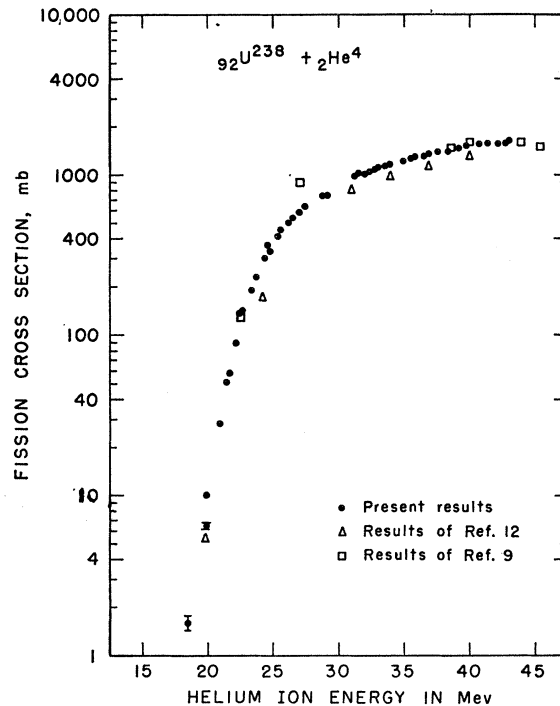
section which is 5% larger than the experimental distribution fitted by the least-squares method. For those bombarding energies for which the differential cross sections were measured at only two angles we have interpolated or extrapolated the data of the two bombarding energies for which full angular distributions were measured to give the magnitude of the deviation between the true angular distribution and that given by the two-angle fit to the simple $a+b\cos^2\theta$ distribution.

The fission cross sections of U²³³ and U²³⁸ are plotted as solid circles in Figs. 3 and 4, respectively. The statistical errors due to counting are less than the physical size of the points except for a few low bombarding energies for which the statistical error flags are shown. The fission cross sections plotted in Figs. 3 and 4 were measured during four different periods of time and during each period some measurements were made at widely different bombarding energies. The radiochemical data of Colby[12] et al. are plotted in Figs. 3 and 4 as triangles and that of Vandenbosch,[9] et al. as squares. Aside from the earlier discussion in the Introduction, no explanation can be given at this time for the consistent trend of the present results to be approximately 15% larger than those of Colby et al.

The sum of the errors introduced into the fission cross section due to uncertainties in target thickness, integrated beam current, detector, solid angle, and fission fragment anisotropy is thought to be less than 5% for U²³⁸. The comparable error for U²³³ is approximately

10% since these targets have small irregularities in their thicknesses.

The quality of the degraded beam in terms of energy spread is related to the energy spread of the emergent beam and the straggling introduced by the absorber foil which is used in reducing the energy of the emergent beam. The energy spread of the degraded deuteron beam from the Argonne cyclotron has been measured[14] as a function of energy but no similar study has been made for helium ions. Preliminary measurements,[16] however, indicate that the emergent beam of helium ions (43 Mev) has an energy spread with a full width at half-maximum intensity of about 0.4 Mev. The energy spread of the helium ion beam at various energies has been determined by combining the energy spread of the emergent beam with calculated values[17] of the energy spread introduced by the energy loss in the aluminum absorbers. From such a calculation, for example, one obtains a full width at half-maximum intensity for 20-Mev helium ions (a most probable energy loss of 23 Mev) of 0.67 Mev. Combining this energy spread with the energy spread of the emergent beam gives a full width at half-maximum intensity of 0.8 Mev for the 20-Mev helium-ion beam.

The fission cross sections in Figs. 3 and 4 are calculated on the basis that the helium ions have a mono-energetic energy equal to that of the mean value of the energy distribution. The magnitude of the error introduced in the fission cross section by this procedure is related to the cross-section dependence on projectile energy as well as the projectile energy distribution. If we assume the energy distribution of the 20-Mev helium ions is Gaussian with a full width at half-maximum intensity of 0.8 Mev, the true cross section is about 5% smaller than the value calculated with the above mentioned assumptions. For higher bombarding energies, both the variation of cross section with energy and energy spread are less, and hence, the errors introduced by assuming a monoenergetic beam are smaller and usually negligible compared to the statistical errors.

As mentioned earlier, in some of the long runs the projectile energy changed enough to alter the range by 1 mg Al/cm². This amounts to an energy uncertainty of about $\frac{1}{4}$ Mev for helium ions degraded to 20 Mev. The mean ranges of the helium ions were converted to energy by the range-energy relation[15] mentioned in the section on experimental procedure.

The strong dependence of the fission cross section on helium ion energy in the vicinity of 20 Mev indicates that the correction for neutron-induced fission is rather small. One expects that the neutron background for small changes in the helium ion energy would be essentially constant, whereas the fission counting rate decreases approximately a factor of 5 for a 1-Mev decrease in helium-ion energy. The following experiment was

[16] T. Braid (private communication).
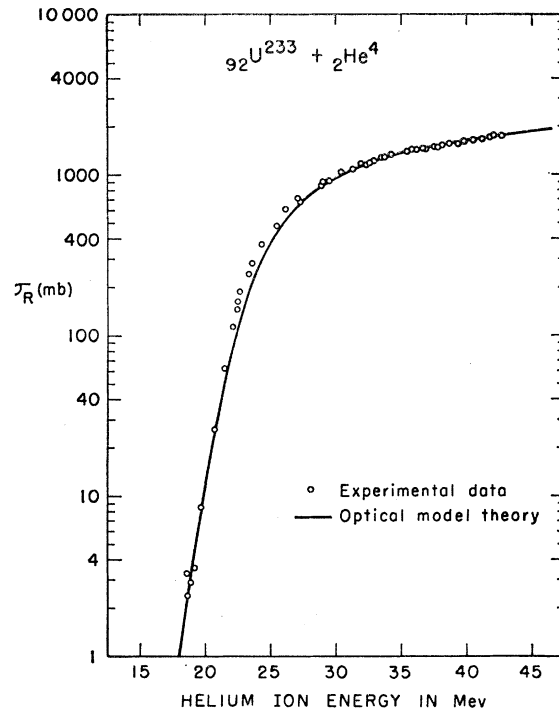[17] T. E. Cranshaw, *Progress in Nuclear Physics* Vol. 2 (Pergamon Press, New York, 1952), Vol. 2, p. 271.

FIG. 5. Comparison of experimental and theoretical total reaction cross sections of U^{233}. The theoretical cross sections are those obtained with an optical model program with a nuclear potential of the Woods-Saxon form, $(V+iW)/\{1+\exp[(r-r_0)/d]\}$. The parameters V, W, r_0, and d were chosen to reproduce the complex potential determined by Igo [Eq. (1)] for values of r where the absolute value of the real part of the potential is less than 10 Mev.

done to accentuate the neutron background and check the influence of neutrons on the fission counting rate. The beam energy was reduced to 22 Mev with aluminum foils in the degrading system[14] which is located near the cyclotron. The fission cross section of U^{233} was then measured for 19-Mev helium ions which were produced with two different absorber systems. In the first arrangement additional absorber was introduced in the degrading system. In the second arrangement an equivalent amount of absorber was introduced at the entrance to the scattering chamber (located in the experimental area and many meters from the degrading system) in order to reduce the energy from 22 to 19 Mev and at the same time enhance the effect of neutrons. For each of the absorber arrangements the fission cross section decreased a factor of about 40 and therefore, within our experimental accuracy the neutrons were not inducing fission.

The reaction cross sections of U^{233} and U^{238} were obtained by adding to the fission cross sections the previously measured values of the spallation cross sections.[9,18] At a helium-ion bombarding energy of 43 Mev the spallation cross section represents about 4 and 9% of the reaction cross sections of U^{233} and U^{238}, respectively. Included in the U^{233} spallation cross sections

[18] J. Wing, W. J. Ramler, A. L. Harkness, and J. R. Huizenga, Phys. Rev. 114, 163 (1959).

are the U²³³ ($\alpha,\alpha n$) cross sections which are deduced from systematics[19], on the competition of fission to neutron emission to be approximately one-half the magnitude of the measured U²³⁸ ($\alpha,\alpha n$) cross sections. At a bombarding energy of 25 Mev the spallation cross section represents about 1 and 14% of the reaction cross sections of U²³³ and U²³⁸, respectively. The reaction cross sections of U²³³ and U²³⁸ are plotted as a function of helium ion bombarding energy in the laboratory system in Figs. 5 and 6, respectively. The magnitudes of the cross sections for the two different targets are equal within the experimental errors.

DISCUSSION

The optical model program which was used in calculating the reaction cross sections required a nuclear potential of the Woods-Saxon form,

$$(V+iW)\Big/\left[1+\exp\!\left(\frac{r-r_0}{d}\right)\right].\qquad(2)$$

The parameters V, W, r_0 and d were chosen to reproduce the complex potential given in Eq. (1) for values of r where the absolute value of the real part of the potential
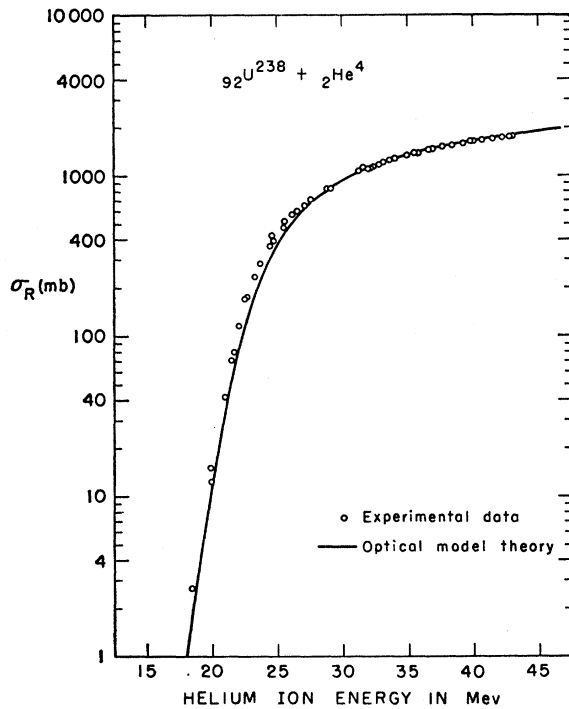

FIG. 6. Comparison of experimental and theoretical total reaction cross sections of U²³⁸. The theoretical cross sections are those obtained with an optical model program with a nuclear potential of the Woods-Saxon form, $(V+iW)/\{1+\exp[(r-r_0)/d]\}$. The parameters V, W, r_0, and d were chosen to reproduce the complex potential determined by Igo [Eq. (1)] for values of r where the absolute value of the real part of the potential is less than 10 Mev.

[19] R. Vandenbosch and J. R. Huizenga, *Proceedings of the Second United Nations International Conference on the Peaceful Uses of Atomic Energy* (United Nations, Geneva, 1958), Vol. 15, p. 1688, p. 284.
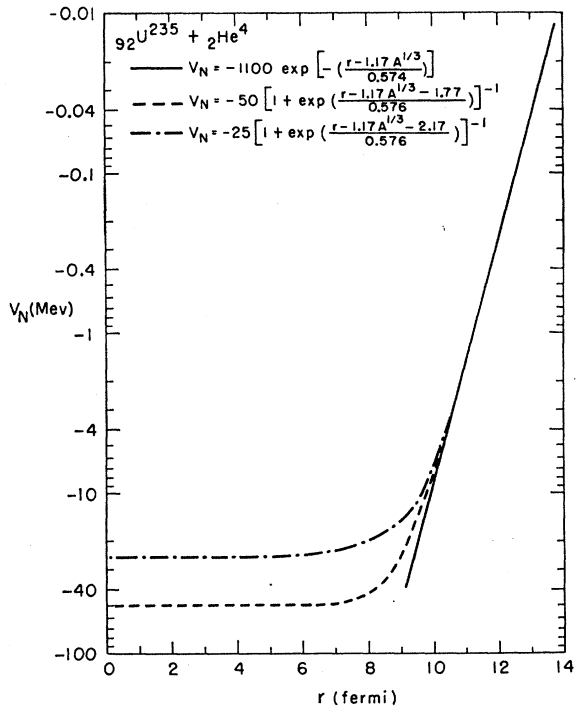

FIG. 7. Comparison of the real potential of Igo with those obtained for two different sets of Woods-Saxon parameters, ($V=-50$ Mev, $r_0=8.99$ fermi, and $d=0.576$ fermi) and ($V=-25$ Mev, $r_0=9.39$ fermi, and $d=0.576$ fermi). The magnitudes of the three potentials are similar for $r>10$ fermi.

is less than 10 Mev. With the above parameters fixed, the depth of the potential for small values of r is also fixed although the alpha-particle scattering and total cross sections are not sensitive to the potential depth.

Curves representing the real part of the optical potential derived with Eq. (2) for two different sets of Woods-Saxon parameters, namely $V=-50$ Mev, $r_0=8.99$ fermi, $d=0.576$ fermi and $V=-25$ Mev, $r_0=9.39$ fermi, $d=0.576$ fermi, are plotted along with the real potential of Igo [Eq. (1)] in Fig. 7. For values of r beyond the nuclear radius, the real potentials given by the three equations are approximately equal. From a similar type of graph for the imaginary potential, one concludes that the imaginary potential of Igo is equally well reproduced for comparable r values by the following two sets of Woods-Saxon parameters, $W=-27$ Mev, $r_0=8.99$ fermi, and $d=0.576$ fermi; and $W=-13.9$ Mev, $r_0=9.39$ fermi, and $d=0.576$ fermi.

The optical-model total-reaction cross sections which are plotted in Figs. 5 and 6 as solid lines have been calculated[20] with the Woods-Saxon parameters $V=-50$ Mev, $W=-27$ Mev, $r_0=8.99$ fermi, and $d=0.576$ fermi. The alternate set of parameters, $V=-25$ Mev, $W=-13.9$ Mev, $r_0=9.39$ fermi, and $d=0.576$ fermi, give reaction cross sections which agree with the values from the above set to within 1%. Even though the depths of the two complex potentials given by the two sets of parameters are quite different for small values of

[20] J. R. Huizenga and G. Igo (unpublished results).

r, they are quite similar for large values of r. Since absorption occurs in the surface region, the magnitude of the complex potential in this region is the critical factor in determining the reaction cross section.

The agreement between the experimental and optical model reaction cross sections is in general quite good. In order to get comparable agreement between the experimental cross section values and those predicted with the square-well model of Weisskopf[21] an interaction radius of 11.2 fermi is required. Values of this magnitude[22,23] for the radii of heavy elements are usually obtained with sharp-cutoff models which measure the alpha-particle interactions with nuclei. The value of the radius r_0 in the optical model with a diffuse potential, which has a form factor for the real and imaginary potentials given by Eq. (2), is defined as the distance at which the nuclear potential has fallen to half its central value. With the Woods-Saxon parameters $V = -50$ Mev, $W = -27$ Mev, $r_0 = 8.99$ fermi, and $d = 0.576$ fermi, the absolute value of the potential has decreased a factor of 10 at $r = 10.3$ fermi, i.e., $V + iW = (-5 - i2.7)$ Mev. The real potential is about -0.8 Mev at $r = 11.2$ Mev, whereas the imaginary potential at the same radius is about -0.4 Mev. The alpha particle–nuclear potential of the optical model is probably larger than the matter distribution of the nucleus due to the alpha-particle size, finite range of the nuclear forces and other details which contribute to the extension of the potential.

There is some indication from neutron and proton scattering experiments that the depth of the real potential decreases with increasing energy. From analyses of alpha-particle scattering, however, this trend has not been observed. In the calculation of the optical-model cross sections which are plotted in Figs. 5 and 6 we have assumed that the Woods-Saxon parameters are energy independent. One of the justifications for this assumption is that the absorption of alpha particles by nuclei is so strong that the absorption length is only about 1×10^{-13} cm and most partial waves do not experience the real part of the potential lying within the nucleus.

The experimental total reaction cross sections with 20- to 27-Mev helium ions are slightly larger than the values derived from optical model theory with the Woods-Saxon parameters based on the Igo potential, whereas the agreement at higher energies is very good (the experimental cross sections are not well determined for energies less than 20 Mev). One way to bring the theoretical cross sections into better agreement with the experimental values is to use an energy-dependent real potential. For example, if the real potential is given by $V = (-109 + 1.56 E)$ Mev ($V = -50$ and -75 Mev for 38-Mev and 22-Mev helium ions on uranium, respec-

tively) and the other Woods-Saxon parameters are kept fixed at $W = -27$ Mev, $r_0 = 8.99$ fermi, and $d = 0.576$ fermi, the optical-model cross sections have an energy dependence more comparable to the experimental results. Increasing the depth of the real potential from -50 to -75 Mev for 22-Mev helium ions increases the reaction cross section at this energy by 30%.

The use of an energy-dependent real potential is not a unique solution for obtaining improved agreement between the theoretical and experimental energy dependence of the reaction cross section. Many other combinations of Woods-Saxon parameters also have comparable effects even though one limits the possibilities by using the same form factor for both the real and imaginary potentials. Changes in the Woods-Saxon parameters which increase the depth of the real or imaginary (or both) potential in the radial region of $r > 10$ fermi (see Fig. 7) increase the reaction cross sections for lower bombarding energies by a larger percentage than the higher bombarding energies. Likewise if one changes the slope of the real and imaginary potentials for $r > 10$ fermi by changing the diffuseness parameter d, one effects a larger change in the cross sections for smaller bombarding energies. For example, the two sets of Woods-Saxon parameters ($V = -50$ Mev, $W = -27$ Mev, $r_0 = 8.99$ fermi, and $d = 0.576$ fermi) and ($V = -42.27$ Mev, $W = -22.82$ Mev, $r_0 = 8.99$ fermi, and $d = 0.65$ fermi) give the same complex potential at $r = 10$ fermi, namely $(-7.38 - i3.99)$ Mev. The cross sections calculated with the latter set of parameters, however, are 40%, 10%, and 6% higher for 22-, 30-, and 38-Mev helium ions, respectively.

The complex potential of Eq. (1) was deduced from analyses[2] of elastic-scattering data for 18-Mev alpha particles from argon, 40-Mev alpha particles from copper, and 48-Mev alpha particles from lead. Comparable analyses should be made for uranium in order to utilize the uranium-reaction cross sections most effectively in checking the optical-model theory. The nonspherical nuclear shape of uranium may also be of some importance. The magnitude of the uncertainty in the complex potential given by Eq. (1) can be estimated from the figures in reference 2. For example, one deduces from Fig. 12 of reference 2 that the imaginary parts of the nuclear potential for two "best fits" of the elastic scattering data for 48-Mev alpha particles on lead differ in the critical region of the radius by a factor of 2. The dependence of the optical model cross section on changes in the complex potential has been discussed[20] elsewhere. Within the uncertainties in the complex alpha particle-nuclear potential, the present experimental cross sections are in agreement with the optical model predictions.

[21] J. M. Blatt and V. F. Weisskopf, *Theoretical Nuclear Physics* (John Wiley & Sons, Inc., New York, 1952), p. 352.
[22] J. O. Rasmussen, Revs. Modern Phys. **30**, 424 (1958).
[23] D. D. Kerlee, J. S. Blair, and G. W. Farwell, Phys. Rev. **107**, 1343 (1957).